GROUND-BASED OBSERVATIONS OF THERMOSPHERIC/IONOSPHERIC WAVES AND LOW-LATITUDE AURORAS USING ALL-SKY COOLED-CCD IMAGERS

НАЗЕМНЫЕ НАБЛЮДЕНИЯ ЗА ТЕРМОСФЕРНЫМИ / ИОНОСФЕРНЫМИ ВОЛНАМИ И ЗА НИЗКОШИРОТНЫМ СВЕЧЕНИЕМ АТМОСФЕРЫ С ПОМОЩЬЮ ПАНОРАМНЫХ ОХЛАЖДАЕМЫХ ПЗС ФОТОПРИЕМНИКОВ

K. Shiokawa, Y. Otsuka, and T. Ogawa

Solar-Terrestrial Environment Laboratory, Nagoya University, Toyokawa, 442-8507, Japan

Мы запустили девять панорамных ПЗС камер в Японии (на 4 станции), Австралии (1 станция), Индонезии (1 станция), Канаде (2 станции) и в США (1 станция), которые являются частью оптических фотоприемников для наблюдения за мезосферой и термосферой (OMTI, http://stdb2.stelab.nagoya-u.ac.jp/omti/index.html). Фотоприемники измеряют излучение свечения атмосферы на следующих длинах волн: 557.7 нм (кислород, высота: 90-100 км), 630.0 нм (кислород, 200-300 км), и 720-910 нм (излучение полосы гидроксила, 80-90 км). При измерениях с помощью фотоприемника можно получить двух пространственные изображения гравитационных волн небольшой шкалы (менее 100 км) в области мезопаузы, перемещающиеся ионосферные возмущения средней и большой шкалы в термосфере/ионосфере, и явления свечения атмосферы на низких широтах во время магнитных бурь. В этом докладе мы даем обзор характерных черт этих волн и свечений атмосферы, которые наблюдаются с помощью фотоприемников. Мы также представляем наш план установки новых фотоприемников и индукционных магнитометров на Дальнем Востоке России в сотрудничестве с Институтом космофизических исследований и распространения радиоволн (ИКИР) ДВО РАН.

1. Introduction

The Earth's atmosphere at high altitudes (above 80 km) emits weak light at night at several line wavelengths. They are called nocturnal airglow. Figure 1 shows a schematic picture of the typical airglow emission layers and their relations to the atmospheric temperature and ionospheric ion density.

The oxygen green line at a wavelength of 557.7 nm and hydroxyl (OH) band emissions (many lines at near-infrared wavelengths) have airglow layers near the mesopause region, where the atmospheric temperature is lowest in the Earth's atmosphere. Since the electron density is very low at this altitude range, the variations of these airglow emissions are controlled by variations in the atmosphere, mostly due to atmospheric gravity waves. The emission of oxygen red line at a wavelength of 630.0 nm comes from the lower thermosphere at altitudes of 200-300 km. Since this emission is basically excited by interactions of oxygen ion (O^+) and molecular oxygen (O_2) (e.g, Sobral et al., 1993), the intensity of 630-nm airglow is a sensitive indicator to the changes in ionospheric ion density and in the height of the ionosphere. By using highly-sensitive all-sky imagers with cooled charge coupled device (CCD) cameras and narrow band-pass filters, one can obtain two-dimensional images of these airglow emissions and hence the atmospheric and ionospheric variations.

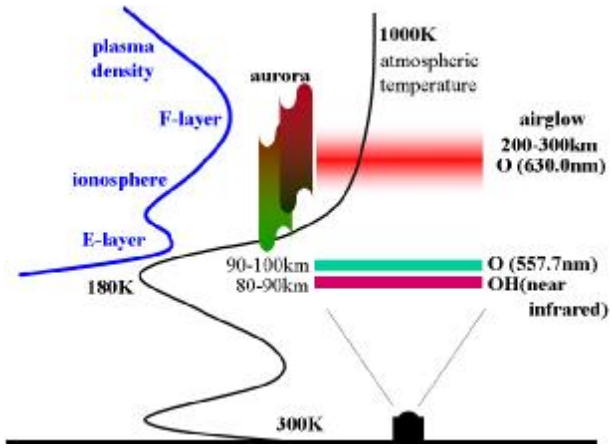

Fig.1. Schematic pictures of the three airglow layers, aurora, atmospheric temperature profile, and ionospheric ion density profile.

2. The Optical Mesosphere Thermosphere Imagers (OMTIs)

The Optical Mesosphere Thermosphere Imagers (OMTIs) have been made airglow imaging observations since 1997 (Shiokawa et al., 1999). The OMTIs consist of all-sky imagers, a Fabry-Perot interferometer, meridian scanning photometers, and airglow temperature photometers. In this paper we mostly focus on the results obtained by the all-sky imagers. The imager uses thinned and back-illuminated cooled-CCD with 512x512 pixels. All the OMTIs imagers have at least four filters on a wheel to measure 557.7-nm, 630.0-nm and OH-band emissions, and sky background emissions at 572.5 nm. The time resolution and exposure times to obtain these emissions are ~2-5 min and 10-165 s, respectively. Some imagers have additional filters to measure emissions from thermospheric oxygen (777.4 nm), mesospheric sodium (589.3 nm) and auroral oxygen (844.6 nm) and hydrogen (486.1 nm). The bandwidths of the band-pass filters for the measurement are ~1.5-2.0 nm. For details of the imagers, please see Shiokawa et al. (2000).

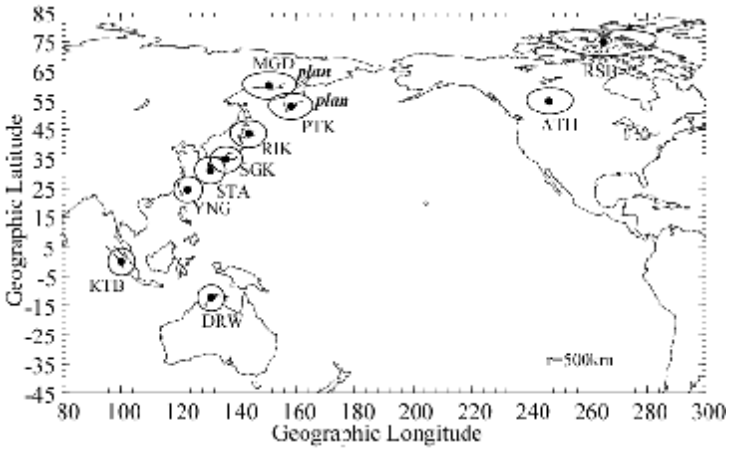

Fig.2. Stations of the Optical Mesosphere Thermisphere Imagers (OMTIs). The imager at YNG belongs to the Electronic Navigation Research Institute (ENRI).

The imagers and other optical instruments have been installed at various places in the world. Figure 2 shows the current and planned stations of all-sky imagers. Table 1 lists the latitudes and longitudes of the stations. The imager at Resolute Bay (RSB) measures sun-aligned auroral arcs and polar cap patches (Hosokawa et al., 2006). The imagers at Athabasca (ATH) measures auroras at subauroral latitudes (Sakaguchi et al., 2007). The imagers at mid- and low-latitudes in Japan (RIK, SGK, STA, and YNG), Indonesia (KTB), and Australia (DRW) measures atmospheric gravity waves in the mesopause region and traveling ionospheric disturbances and plasma bubbles in the thermosphere/ ionosphere through the airglow emissions in Figure 1.

station	abbr.	geographic latitude	geographic longitude	magnetic latitude	inclination (degree)	declination (degree)	observation period
Resolute Bay	RSB	74.7	265.1	82.9	88.1	32.1	Jan 2005
Athabasca	ATH	54.7	246.7	61.7	76.6	17.4	Sep 2005-
Magadan	MGD	60.0	150.9	51.9	71.5	-11.1	planned
Paratunka	PTK	52.9	158.3	45.7	64.5	6.5	planned
Rikubetsu	RIK	43.5	143.8	34.9	57.4	-8.9	Oct 1998-
Shigaraki	SGK	34.8	136.1	25.6	48.6	-7.0	Oct 1998-
Sata	STA	31.0	130.7	21.5	41.1	-5.9	Jul 2000-
Yonaguni	YNG	24.5	123.0	14.6	35.1	-3.6	Mar 2006-
Kototabang	KTB	-0.20	100.3	-10.4	-13.8	-0.3	Oct 2002-
Darwin	DRW	-12.4	131.0	-21.8	-38.9	3.5	Oct 2001-

Table 1. List of stations shown in Figure 2. Geomagnetic values are calculated using the IGRF-10 mode at epoch 2005 at an altitude of 0 km.

3. Some images obtained by OMTIs

Figure 3 shows typical examples of airglow and auroral images obtained by the imagers of OMTIs. The top left panel shows the gravity waves in the mesopause region observed by the all-sky imager at Shigaraki, Japan at 14:05 UT (23:05 LT) on May 20, 2007 with an exposure time of 15 s. The gravity wave was seen in the OH-band images (emission altitudes: 80-90 km). The wave has phase front of ESE-WNW with a wavelength of ~20-30 km propagate toward NNE throughout the night.

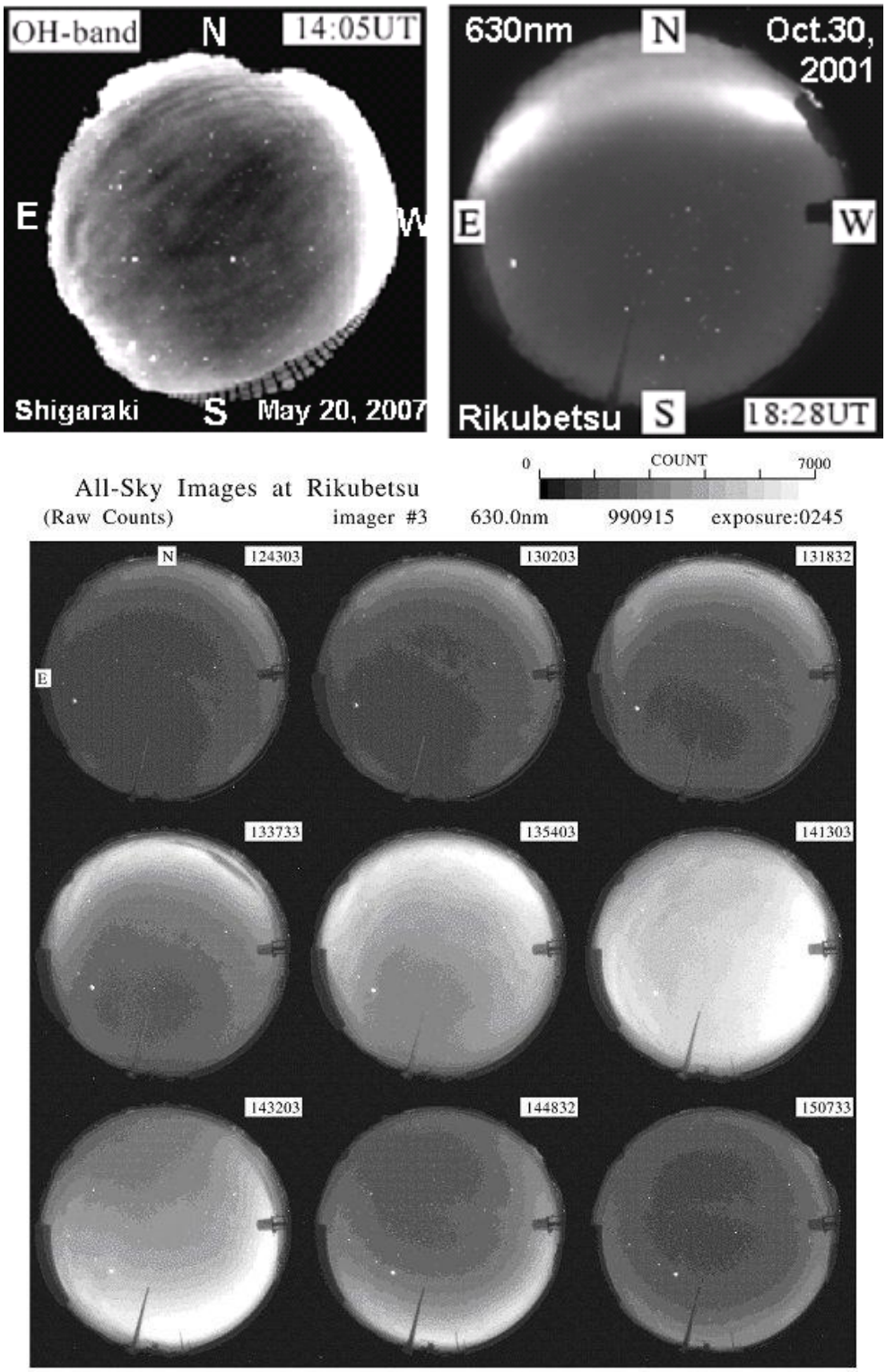

Fig.3. Typical airglow/aurora images obtained by the imagers of OMTIs. Top left: gravity wave in the mesopause region, top right: low-latitude red aurora during a geomagnetic storm, and bottom nine panels: large-scale traveling ionospheric disturbance during a geomagnetic storm.

The top right panels of Figure 3 is an event of low-latitude red aurora observed at Rikubetsu, Japan at 18:28 UT (03:28 LT) during the severe geomagnetic storm of October 30, 2001. The aurora in red (630-nm) emission approached to Rikubetsu from the northern horizon, as the storm develops. Using this highly-sensitive all-sky imager, we have succeeded to observe 20 events of low-latitude red auroras in Japan during the last solar maximum of 1999-2004. Details of these observations were reported by Shiokawa et al. [2005].

The bottom nine images in Figure 3 show a passage of large-scale traveling ionospheric disturbance from north to south during the moderate geomagnetic storm of September 15, 1999 (Shiokawa et al., 2002). During geomagnetic storms, we often observe such large scale (>~1000

km) ionospheric waves in the 630-nm airglow images (e.g., Shiokawa et al., 2003; 2007). They are probably large scale atmospheric waves in the thermosphere caused by auroral energy input to the high latitude auroral zone and propagating to lower latitudes.

4. Observation plan in far-eastern Russia

As shown by the examples in the previous section, OMTIs are capable of imaging various atmospheric/ionospheric waves and auroras. These waves are indications of energy flow from space into the high-altitude atmosphere and propagation of the energy to lower latitudes. In order to connect the disturbances at high latitudes to those at low latitudes, such as Japan, we plan to install two imagers in far-eastern Russia in collaboration with the Institute of Cosmophysical Research and Radiowave Propagation (IKIR), Far Eastern Branch of the Russian Academy of Sciences. Figure 4 is a schematic diagram showing the configurations of measurements. As shown in Figure 2, we plan to install two all-sky airglow/auroral imagers in the far-eastern Russia. The aurora, storm-time red aurora at lower latitudes, and thermospheric waves produced by auroral energy input and by other atmospheric/ionospheric disturbances, can be monitored by the chain of all-sky imagers. These imaging measurements will be combined with other related measurements, such as (1) SuperDARN HF radar at Rikubetsu, Japan, which has been started routine observations of the plasma drift in the ionosphere since December 2007, (2) GEONET network, which consists of more than 1000 GPS receivers to measure total electron content over Japan, MAGDAS/CPMN/210MM magnetometer networks, and many satellites at the ionospheric and magnetospheric altitudes. These combined measurements will give new insights into dynamics of the upper atmosphere and the ionosphere and their relation to the energy input from the magnetosphere.

Acknowledgements

We thank the Institute of Cosmophysical Research and Radiowave Propagation (IKIR), Far Eastern Branch of the Russian Academy of Sciences, for their support in preparation of the installation of two stations at far eastern Russia. The measurements of OMTIs have been supported by the Grant-in-Aid for Scientific Research (11440145, 13573006, 13136201, 16403007, 18403011, 19403010, and Priority Area 764) and Dynamics of the Sun-Earth-Life Interactive System (No.G-4, the 21st Century COE Program) of the Ministry of Education, Culture, Sports, Science and Technology of Japan.

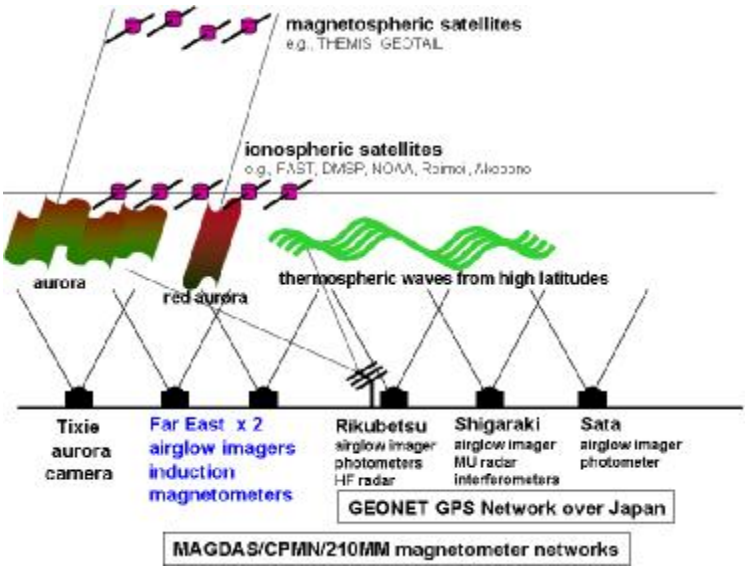

Fig.4. Schematic diagram showing the configuration of the measurements using stations in Japan and far-eastern Russia.

References

1. Hosokawa, K., K. Shiokawa, Y. Otsuka, A. Nakajima, T. Ogawa, and J. D. Kelly, Estimating drift velocity of polar cap patches with all-sky airglow imager at Resolute Bay, Canada, Geophys. Res. Lett., 33, L15111, doi:10.1029/2006GL026916, 2006.
2. Sakaguchi, K., K. Shiokawa, A. Ieda, Y. Miyoshi, Y. Otsuka, T. Ogawa, M. Connors, E. F. Donovan, and F. J. Rich, Simultaneous ground and satellite observations of an isolated proton arc at subauroral latitudes, J. Geophys. Res., 112, A04202, doi:10.1029/2006JA012135, 2007.
3. Shiokawa, K., Y. Katoh, M. Satoh, M. K. Ejiri, T. Ogawa, T. Nakamura, T. Tsuda, R. H. Wiens, Development of optical mesosphere thermosphere imagers (OMTI), Earth Planets Space, 51, 887-896, 1999.
4. Shiokawa, K., Y. Katoh, M. Satoh, M. K. Ejiri, and T. Ogawa, Integrating-sphere calibration of all-sky cameras for nightglow measurements, Adv. Space Sci., 26, 1025-1028, 2000.
5. Shiokawa, K., Y. Otsuka, T. Ogawa, N. Balan, K. Igarashi, A. J. Ridley, D. J. Knipp, A. Saito, and K. Yumoto, A large-scale traveling ionospheric disturbance during the magnetic storm of September 15, 1999, J. Geophys. Res., 107(A6), 10.1029/2001JA000245, 2002.
6. Shiokawa, K., Y. Otsuka, T. Ogawa, S. Kawamura, M. Yamamoto, S. Fukao, T. Nakamura, T. Tsuda, N. Balan, K. Igarashi, G. Lu, A. Saito, and K. Yumoto, Thermospheric wind during a storm-time large-scale traveling ionospheric disturbance, J. Geophys. Res., 108(A12), 1423, doi:10.1029/2003JA010001, 2003.
7. Shiokawa, K., G. Lu, Y. Otsuka, T. Ogawa, M. Yamamoto, N. Nishitani, and N. Sato, Ground observation and AMIE-TIEGCM modeling of a storm-time traveling ionospheric disturbance, J. Geophys. Res., 112, A05308, doi:10.1029/2006JA011772, 2007.
8. Shiokawa, K., T. Ogawa, and Y. Kamide, Low-latitude auroras observed in Japan: 1999-2004, J. Geophys. Res., 110, A05202, doi:10.1029/2004JA010706, 2005.
9. Sobral, J. H. A., H. Takahashi, M. A. Abdu, P. Muralikrishna, Y. Sahai, C. J. Zamlutti, E. R. DE Paura, and P. P. Batista, Determination of the quenching rate of the $O(^1D)$ by $O(^3P)$ from rocket-borne optical (630 nm) and electron density data, J. Geophys. Res., 98, 7791-7798, 1993.